Suppression of space charge in crosslinked polyethylene filled with poly(stearyl methacrylate)-grafted SiO_2 nanoparticles

Ling Zhang, Mohammad M. Khani, Timothy M. Krentz, Yanhui Huang, Yuanxiang Zhou, Brian C. Benicewicz, J. Keith Nelson, and Linda S. Schadler

Citation: Appl. Phys. Lett. **110**, 132903 (2017); doi: 10.1063/1.4979107
View online: http://dx.doi.org/10.1063/1.4979107
View Table of Contents: http://aip.scitation.org/toc/apl/110/13
Published by the American Institute of Physics

Suppression of space charge in crosslinked polyethylene filled with poly(stearyl methacrylate)-grafted SiO_2 nanoparticles

Ling Zhang,[1] Mohammad M. Khani,[2] Timothy M. Krentz,[3] Yanhui Huang,[3] Yuanxiang Zhou,[1,a)] Brian C. Benicewicz,[2] J. Keith Nelson,[3] and Linda S. Schadler[3,a)]
[1]*State Key Laboratory of Control and Simulation of Power Systems and Generation Equipments, Department of Electrical Engineering, Tsinghua University, Beijing 100084, China*
[2]*Department of Chemistry and Biochemistry, University of South Carolina, 541 Main Street, Horizon I Room 232, Columbia, South Carolina 29208, USA*
[3]*Department of Materials Science and Engineering, Rensselaer Polytechnic Institute, 110 8th Street MRC 140, Troy, New York 12180, USA*

(Received 5 February 2017; accepted 13 March 2017; published online 29 March 2017)

Incorporating inorganic nanoparticles (NPs) into polymer matrices provides a promising solution for suppressing space charge effects that can lead to premature failure of electrical insulation used in high voltage direct current engineering. However, realizing homogeneous NP dispersion is a great challenge especially in high-molecular-weight polymers. Here, we address this issue in crosslinked polyethylene by grafting matrix-compatible polymer brushes onto spherical colloidal SiO_2 NPs (10–15 nm diameter) to obtain a uniform NP dispersion, thus achieving enhanced space charge suppression, improved DC breakdown strength, and restricted internal field distortion ($\leq$10.6%) over a wide range of external DC fields from −30 kV/mm to −100 kV/mm at room temperature. The NP dispersion state is the key to ensuring an optimized distribution of deep trapping sites. A well-dispersed system provides sufficient charge trapping sites and shows better performance compared to ones with large aggregates. This surface ligand strategy is attractive for future nano-modification of many engineering insulating polymers. *Published by AIP Publishing.*
[http://dx.doi.org/10.1063/1.4979107]

Currently, developing high-performance insulating materials for high voltage direct current (HVDC) applications is still a challenge because of space charge injection and accumulation effects. Crosslinked polyethylene (XLPE) is one of the most common and basic insulating polymers used in HV extruded power cables but encounters severe space charge problems under DC conditions due to its high volume resistivity and low carrier mobility.[1] This issue has stimulated investigations into minimizing space charge effects via modifications of the metal/polymer interface and bulk polymer properties.[2–4] Inorganic nanoparticles (NPs) are widely utilized to fabricate polymer nanocomposites (NCs) and nanofillers are believed to provide carrier trapping sites which decrease the overall energy of the carriers and increase the breakdown strength (BDS).[5,6] To achieve optimized properties, the fillers must be well dispersed. However, despite some success in creating improved nanodielectrics by treating NPs with small-molecular coupling agents,[7–9] agglomeration often occurs.[10] To improve the NP dispersion, surface ligand engineering of both the enthalpic and entropic compatibility with the matrix is required.[11,12] In this letter, we report the fabrication of a polymer-brush-grafted SiO_2/XLPE nanocomposite system with homogeneous NP dispersion and the microscopic mechanism of suppression of space charge and internal field distortion over a wide range of external DC fields.

Low-density polyethylene (LDPE, CAS 9002-88-4) and dicumyl peroxide (DCP, CAS 80-43-3) were purchased from Sigma Aldrich. Spherical colloidal SiO_2 NPs (10–15 nm diameter, MEK-ST) were from Nissan Chemical Industries. Reversible addition-fragmentation transfer (RAFT) polymerization was adopted to synthesize poly(stearl methacrylate) (PSMA) brushes on the surface of SiO_2 NPs. The activation of RAFT chain-transfer agents and the synthesis of PSMA brushes were reported in detail previously.[13,14] The average molecular weight (45 kg/mol) and the graft density (0.04 chain/nm^2) of PSMA brushes were estimated via gel permeation chromatography and thermogravimetic analysis (TGA), respectively.[15] Free-PSMA chains (69 kg/mol) were also synthesized as a reference. XLPE and XLPE composite films were prepared by compression molding. Briefly, a nanoparticle solution was premixed with LDPE pellets at 1500 rpm for 5 min and then the solvent was removed under a coarse vacuum. Subsequently, melt mixing using a Thermo Haake PolyDrive was conducted at 145 °C for 10 min. DCP (2 wt. %) was then added into the mixture at 115 °C for another 5 min. Crosslinking and compression molding were carried out at 180 °C and 15 MPa for 15 min. The obtained films with a thickness of ~300 μm were used for space charge measurements, and those with ~100 μm were used for DC breakdown strength (BDS) and thermally stimulated depolarization current (TSC) measurements. For comparison, Free-PSMA chains, with the same weight percentage as that of PSMA brushes grafted on SiO_2 NPs, were added to the XLPE matrix, and as-received unmodified SiO_2 (denoted as UN-SiO_2) NPs were mixed using the same procedure. Four groups were prepared in total, denoted as XLPE, UN-SiO_2/XLPE, Free-PSMA/XLPE, and PSMA-SiO_2/XLPE. All film samples were annealed in a vacuum at

a)Authors to whom correspondence should be addressed. Electronic addresses: zhou-yx@tsinghua.edu.cn and schadl@rpi.edu.

70 °C for 24 h, which reduces any volatile component to a negligible level.

Fig. 1(a) presents TGA studies which revealed that PSMA chains decompose at 300–500 °C and occupied ~50 wt. % of the PSMA-SiO_2 NPs. Fig. 1(b) shows Fourier transform infrared spectra (FTIR) evidence of grafting of PSMA brushes on SiO_2 NPs. The absorption bands at 1628 cm^{-1} were assigned to hydroxyl (O−H) bending vibration. The broad absorptions at 1000–1200 cm^{-1} and 802 cm^{-1} were assigned to Si−O stretching vibration. In comparison to UN-SiO_2 NPs, new absorption peaks, i.e., 2924 cm^{-1} and 2855 cm^{-1} (C−H stretching vibration), 1733 cm^{-1}(C=O bending vibration), and 1465 cm^{-1}(C−H bending vibration), appeared in PSMA-SiO_2 NPs, which are consistent with those in the FTIR spectrum of Free-PSMA chains. Figs. 1(c) and 1(d) provide transmission electron microscopy (TEM) observations of NP dispersion to demonstrate the effectiveness of the RAFT polymer-brush-grafting strategy. In Fig. 1(c), severe μm-level agglomerates formed which could be related to the core-core van der Waals attraction of the nanofillers.[10] On the contrary, PSMA-SiO_2 NPs (see white circles in Fig. 1(d)) exhibited relatively homogeneous distribution of small agglomerates (smaller than 100 nm), which indicates an increase in interfacial volume.

Space charge distribution under −30 kV/mm was examined using a pulsed electro-acoustic method at room temperature (RT) shown in Fig. 2. Immediately after polarization, net positive charges were observed in all samples with a decrease in the positive net charge on the anode.[12,16] After being polarized for 30 min in XLPE (see Fig. 2(a)), net positive charge is distributed across the sample. ~7 C/m^3 of positive carriers advanced and accumulated in the bulk of UN-SiO_2/XLPE NCs. In contrast, Free-PSMA/XLPE composites show a smaller quantity of positive carriers and ~1 C/m^3 of positive carriers gradually accumulated near the cathode during polarization. However, there is no detectable charge in the bulk of PSMA-SiO_2/XLPE NCs after 60 min.

To further demonstrate the ability of the nanocomposites to suppress space charge, a −100 kV/mm field was applied, which was high enough to trigger the critical onset field for charge packets,[17] and the resulting 2-D space charge patterns are presented in Fig. 3. It must be emphasized that cross-linking byproducts and other volatile chemicals can be ruled out by degassing and thus the space charge behavior can be explained in terms of the physical nature of XLPE and XLPE composites. A positive charge packet of ~50 C/m^3 was generated in XLPE and slowed down during the 60 min transit across the insulation with carrier mobilities ranging from $\sim 1.7 \times 10^{-15}$ to $\sim 1.0 \times 10^{-16}$ $m^2/(V\,s)$, which agrees well with previous reports.[18] A smaller positive charge packet formed in UN-SiO_2/XLPE NCs as well, but slowly moved a distance of ~50 μm. As for Free-PSMA/XLPE in Fig. 3(c), bipolar charge injection and transport were observed initially, followed by the appearance of a negative charge packet which transited and recombined with positive carriers near the anode. In the well-dispersed system (see Fig. 3(d)), penetration of both positive and negative space charge was suppressed, and almost no net charge appears in the bulk.[19]

It is argued here that both positive carrier transport and negative carrier transport are present in the neat XLPE, but the net charge in the bulk is positive. PSMA alone is likely to introduce some chemical defects, e.g., its carbonyl (C=O) group, acting as trapping sites, and is able to suppress the positive carrier transport.[20,21] This explains why under high fields when the electron transport starts to become more significant, the net charge in the Free-PSMA/XLPE becomes negative, as shown in Fig. 3(c). On the other hand, Free-PSMA can provide traps for both positive carriers and electrons from its surface states, but good dispersion is critical to

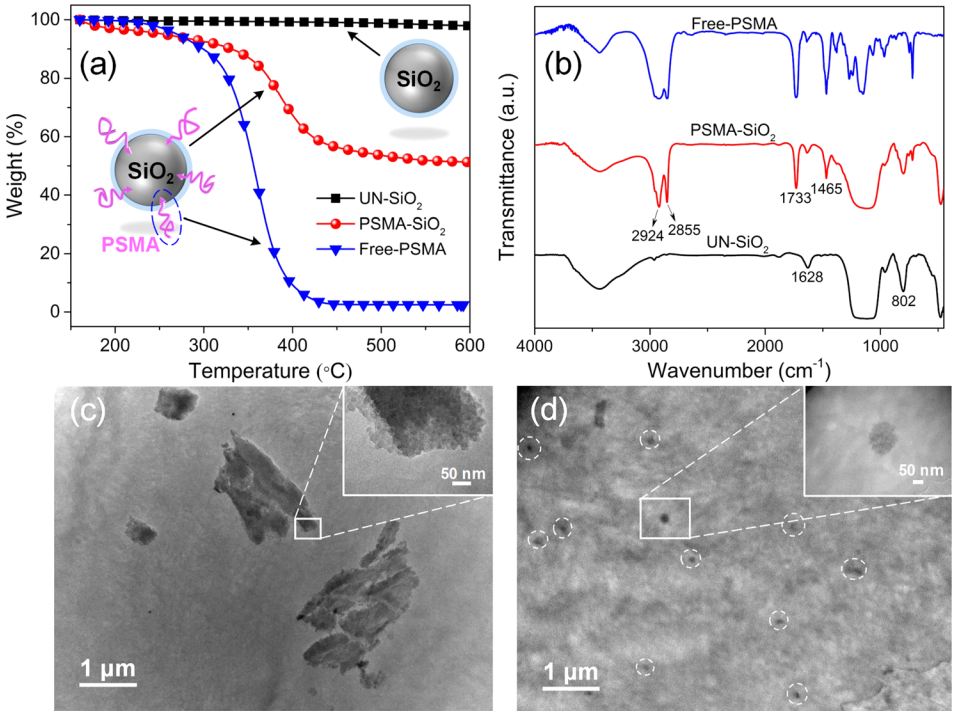

FIG. 1. (a) TGA curves, (b) FTIR spectra, and (c) and (d) are TEM images of UN-SiO_2/XLPE and PSMA-SiO_2/XLPE NCs, respectively.

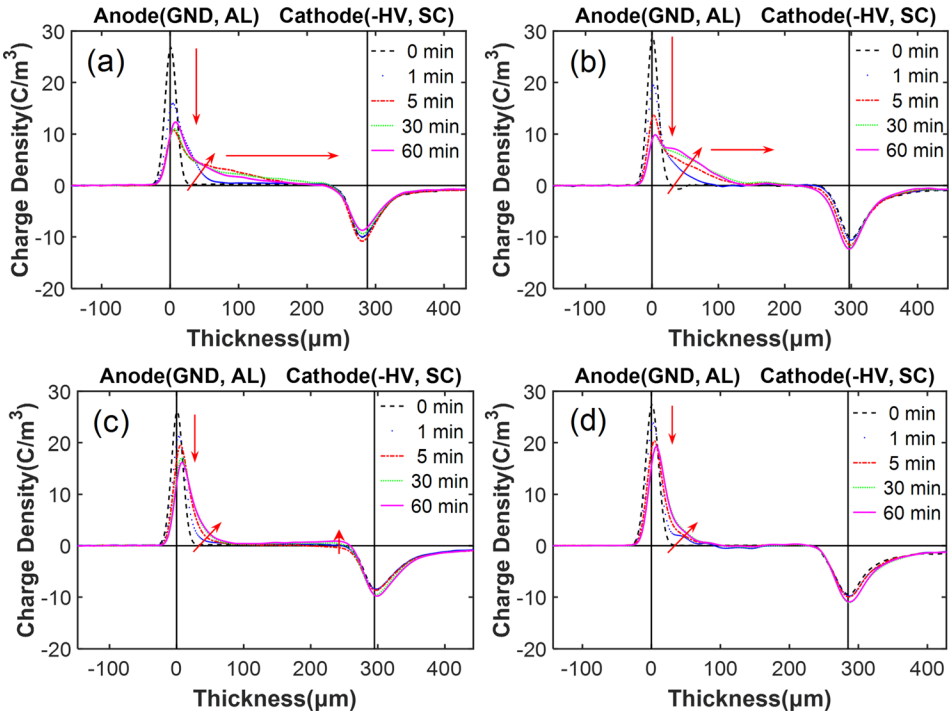

FIG. 2. Space charge distribution under −30 kV/mm in (a) XLPE, (b) UN-SiO_2/XLPE, (c) Free-PSMA/XLPE, and (d) PSMA-SiO_2/XLPE. [AL: aluminum; and SC: semiconductive layer.]

ensure that charges are trapped near the electrode and do not go into the bulk, as shown in Fig. 3(d). TSC measurements were conducted to compare the charge trapping ability of XLPE and XLPE composites, and Fig. 3(e) shows typical TSC spectra. Samples were first polarized under 30 kV/mm at 50 °C for 20 min, and then rapidly cooled down to −70 °C and shorted for 3 min. Afterwards, the temperature was linearly increased with a ramp rate of 5 °C/min. As a widely used semi-crystalline polymer, XLPE has a relatively weak spherulite structure and consists of lamellar stacks compared to the structure of LDPE. The amorphous space accommodates chain branches and ends, cross-linking sites, short polymer chains, etc., and forms physical defects which strongly influence the charge transport process.[22] The TSC

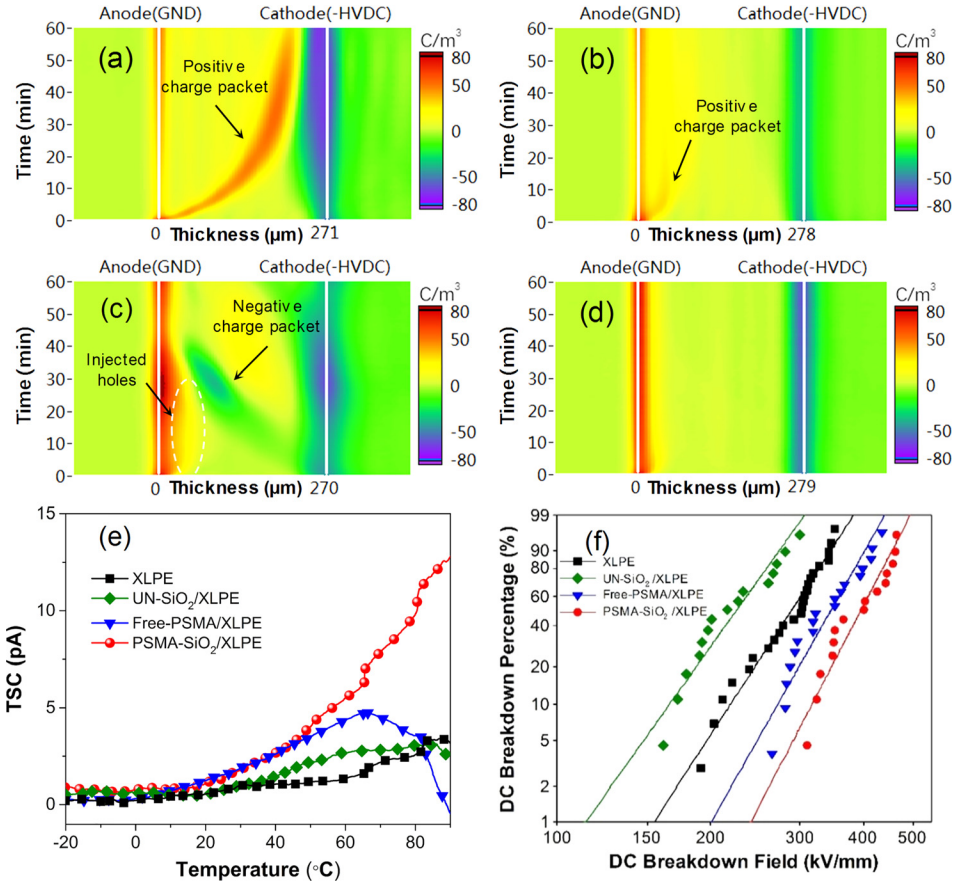

FIG. 3. 2-D space charge patterns under −100 kV/mm in (a) XLPE, (b) UN-SiO_2/XLPE, (c) Free-PSMA/XLPE, and (d) PSMA-SiO_2/XLPE. (e) TSC spectra. (f) Weibull distribution of DC breakdown strength.

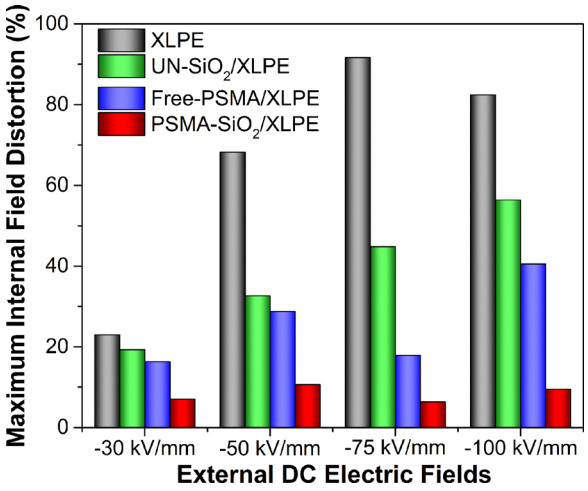

FIG. 4. Maximum internal field distortion under external DC electric fields.

curve of the PSMA-SiO_2/XLPE system showed an exponential growth with the temperature and reached 12.7 pA at 90 °C due to traps in the interfacial region and an increase in the NP-matrix interfacial volume. Furthermore, the large TSC in the well-dispersed system at higher temperature suggests that the newly introduced chemical defects act as deep trapping sites.[23,24] The TSC profile of the highly agglomerated system is very similar or slightly higher compared to the neat XLPE. This result reveals again that distribution of NPs, even as small agglomerates (less than 100 nm) is of critical significance to the ability to suppress space charge for XLPE insulation. Furthermore, the DC breakdown test was carried out with ball-plane electrodes according to International Electrotechnical Commission (IEC) standard 60243-2: 2001 and DC BDS was assessed by the two-parameter Weibull distribution in Fig. 3(f). The results indicate that the agglomerated UN-SiO_2/XLPE system had the lowest breakdown strength, and the relatively well-dispersed system outperformed neat XLPE. Moreover, the addition of Free-PSMA chains did enhance the DC BDS.

Fig. 4 presents the maximum internal field distortion which was deduced from space charge profiles within 60 min at RT. It is clearly shown that neat XLPE encountered a severely increasing trend of field distortion, e.g., 91.6% under −75 kV/mm, due to dramatic charge evolution. Incorporating UN-SiO_2 NPs into XLPE could provide improvement in field distortion but the agglomerates are defects and lead to lower breakdown strengths (see Fig. 3(f)). The Free-PSMA/XLPE group had a better performance than UN-SiO_2/XLPE NCs in terms of the field distortion, which could be related to the introduction of new trapping sites. In particular, the maximum internal field distortion of PSMA-SiO_2/XLPE NCs was only 9.5% even under −100 kV/mm and less than 10.6% over a wide range of DC fields from −30 kV/mm to −100 kV/mm, which shows tremendous potential for improving HVDC power cable insulation.

In summary, we utilized a surface initiated RAFT approach to prepare matrix-compatible PSMA-brush-grafted SiO_2/XLPE NCs with relatively uniform NP distribution of small agglomerates (smaller than 100 nm) and thus achieved a substantial suppression of space charge over a wide range of external DC fields. The relatively uniform NP dispersion state contributes to an increase in interfacial volume and a significant increase in deep trapping sites. The efficient charge trapping ensures that most charges are trapped near the injecting electrode and the field distortion is greatly alleviated. Free-PSMA chains also provide some trapping sites for positive carriers. Our findings support the use of a surface ligand strategy as an effective mean for creating high performance nanodielectrics.

We are grateful for the financial support of State Key Development Program of Basic Research of China (973 Program) (2014CB239501), National Natural Science Foundation of China (50377089), China Postdoctoral Science Foundation (2016M591176), and China Scholarship Council (CSC) (201306210134). We are also grateful for support from the Rensselaer Nanotechnology Center.

[1]M. Fu, L. A. Dissado, G. Chen, and J. C. Fothergill, IEEE Trans. Dielectr. Electr. Insul. **15**(3), 851 (2008).
[2]Z. L. An, Q. Yang, C. Xie, Y. Jiang, F. H. Zheng, and Y. W. Zhang, J. Appl. Phys. **105**, 064102 (2009).
[3]T. J. Lewis, IEEE Trans. Dielectr. Electr. Insul. **1**(5), 812 (1994).
[4]L. Milliere, K. Makasheva, C. Laurent, B. Despax, and G. Teyssedre, Appl. Phys. Lett. **105**, 122908 (2014).
[5]F. Q. Tian, Q. Q. Lei, X. Wang, and Y. Wang, Appl. Phys. Lett. **99**, 142903 (2011).
[6]B. Han, X. Wang, Z. Sun, J. M. Yang, and Q. Q. Lei, Appl. Phys. Lett. **102**, 012902 (2013).
[7]X. Huang, P. Jiang, and Y. Yin, Appl. Phys. Lett. **95**, 242905 (2009).
[8]L. Zhang, Y. X. Zhou, M. Huang, Y. C. Sha, J. H. Tian, and Q. Ye, IEEE Trans. Dielectr. Electr. Insul. **21**(2), 424 (2014).
[9]L. Zhang, Y. X. Zhou, X. Y. Cui, Y. C. Sha, T. H. Le, Q. Ye, and J. H. Tian, IEEE Trans. Dielectr. Electr. Insul. **21**(4), 1554 (2014).
[10]Y. Li, T. M. Krentz, L. Wang, B. C. Benicewicz, and L. S. Schadler, ACS Appl. Mater. Interfaces **6**(9), 6005 (2014).
[11]S. Virtanen, T. M. Krentz, J. K. Nelson, L. S. Schadler, M. Bell, B. Benicewicz, H. Hillborg, and S. Zhao, IEEE Trans. Dielectr. Electr. Insul. **21**(2), 563 (2014).
[12]Y. H. Huang, K. Wu, M. Bell, A. Oakes, T. Ratcliff, N. A. Lanzillo, C. Breneman, B. C. Benicewicz, and L. S. Schadler, J. Appl. Phys. **120**, 055102 (2016).
[13]C. Li, J. Han, C. Y. Ryu, and B. Benicewicz, Macromolecules **39**(9), 3175 (2006).
[14]T. Krentz, M. M. Khani, M. Bell, B. C. Benicewicz, J. K. Nelson, S. Zhao, H. Hillborg, and L. S. Schadler, J. Appl. Polym. Sci. **134**(1), 44347 (2017).
[15]M. Kobayashi, R. Matsuno, H. Otsuka, and A. Takahara, Sci. Technol. Adv. Mater. **7**(7), 617 (2006).
[16]Y. H. Huang and L. S. Schadler, J. Appl. Phys. **120**, 055101 (2016).
[17]L. A. Dissado, in *Proceedings of the 10th IEEE International Conference on Solid Dielectrics* (IEEE, 2010), pp. 1–6.
[18]G. Mazzanti, G. C. Montanari, F. Palmieri, and J. Alison, J. Appl. Phys. **94**, 5997 (2003).
[19]F. Baudoin, R. S. Le, G. Teyssedre, and C. Laurent, J. Phys. D **41**, 025306 (2008).
[20]M. Meunier, N. Quirke, and A. Aslanides, J. Chem. Phys. **115**(6), 2876 (2001).
[21]G. Teyssedre and C. Laurent, IEEE Trans. Dielectr. Electr. Insul. **12**(5), 857 (2005).
[22]J. P. Jones, J. P. Llewellyn, and T. J. Lewis, IEEE Trans. Dielectr. Electr. Insul. **12**(5), 951 (2005).
[23]M. Ieda, IEEE Trans. Electr. Insul. **EI-19**(3), 162 (1984).
[24]F. Q. Tian, W. B. Bu, L. S. Shi, C. Yang, Y. Wang, and Q. Q. Lei, J. Electrostat. **69**(1), 7 (2011).